Open Research Statement:

Data and MATLAB codes for results reported here are available in the Github repository

https://github.com/mshoja/reconstruction-anonymized

Abstract

1. The ecological literature often features phenomenological dynamic models lacking robust validation against observational data. Reverse engineering ecological models from data is an alternative approach, where time series data are utilized to infer or fit a stochastic differential equation. This process, known as system reconstruction, presents significant challenges especially when data resolution is low. This paper addresses the estimation of the (often) non-linear deterministic and stochastic parts of Langevin models from sparsely sampled time series.

2. We introduce a Maximum Likelihood Estimation (MLE) inference method, termed Euler reconstruction, tailored for time series data with high resolution. However, the Euler approach is not reliable for low-resolution data. To fill the gap for sparsely sampled data, we present an MLE inference method pioneered by Aït-Sahalia, that we term Hermite reconstruction. We employ splines to detect inherent nonlinearities in the unknown data-generating system with high accuracy and acceptable computational burden.

3. We applied both methods to a range of simulated, ecological, and climate datasets, with different data resolutions. We provide a practical measure (‘relaxation time’) to distinguish between different data resolutions. For simulated data, we show that the Euler reconstruction can accurately reveal the underlying system when data resolution is high, while Hermite reconstruction can recover the system even with low resolution. We recommend using Hermite reconstruction for real data even when the resolution is relatively high. Only when the resolution of real data is exceptionally high might Euler reconstruction suffice.

4. We provide a MATLAB package and a tutorial to assist researchers in applying the method to their own data.

KEYWORDS

Langevin models, system reconstruction, Data resolution, Euler reconstruction, Hermite reconstruction, spline modeling

Introduction. It has long been a matter of debate whether ecosystems can have alternative stable states (Connell & Sousa 1983; Guarini & Coston-Guarini 2024) and whether there can be critical transitions between these states. These are fundamental ecological questions which have mainly been discussed using theoretical models (Scheffer *et al.* 2001), which typically consists non-linear deterministic equations. These models were often used to predict the kind of dynamics to be expected in field data (Scheffer & Carpenter 2003). Alternatively, deterministic models were calibrated using field data (Janse *et al.* 2010). Recently, some techniques have been developed to infer the equations without prior knowledge on the underlying equations (e.g. symbolic regression (Chen, Angulo & Liu 2019)).

All these techniques ignore the fact that ecological systems are never in equilibrium, but constantly perturbed by a stochastic regime of internal and external perturbations (Bjørnstad & Grenfell 2001). This regime of stochastic perturbations is essential for assessing the long-term resilience of ecosystems, as measured, for example, by the mean exit time (Arani *et al.* 2021). To describe these phenomena, we need to include stochastic processes in the model, which are notoriously hard to parameterize.

Tackling these questions necessitates a reverse engineering approach, where we reconstruct stochastic system based on dynamic data (Siegert & Friedrich 2001; Rinn *et al.* 2016). Subsequently, the resilience of the best-fitting model can be studied (Bolker *et al.* 2013; Hilborn & Mangel 2013; Arani *et al.* 2021). When appropriate mechanistic dynamical equations are known, parameters of the equations can be inferred from time series data.

Ecologists are often confronted with a situation where the nonlinear stochastic model that generated the data is unknown and must be inferred from data. If data are measured frequently throughout the entire range of the state variables, a nonlinear stochastic model can be reconstructed using a widely used nonparametric

method, known in the literature as the 'Langevin approach' (Siegert, Friedrich & Peinke 1998; Bandi & Phillips 2003; Rinn *et al.* 2016). The reconstructed model can then be analyzed to map the stability landscape, locate stable or unstable equilibria, and calculate stochastic indicators of resilience such as mean exit time or median survival time (Arani *et al.* 2021). While Langevin approach is appealing, it has several limitations. It requires high-resolution data and involves arbitrary choices, such as estimating the conditional mean, conditional variance, and higher conditional moments using kernels with bandwidths that control smoothness. Estimating the bandwidth is challenging, and the results may be sensitive to its choice. Additionally, this method extrapolates the conditional expectation and variability of the rate of change in data to zero for few time lags (Siegert & Friedrich 2001; Bandi & Phillips 2003; Rinn *et al.* 2016). The choice of the number of lags significantly affects the results, particularly when data resolution is low. Other inference techniques involve Bayesian methods where the specification of appropriate prior can be a delicate matter (Freedman 1963; Freedman 1965; Golightly & Wilkinson 2011; Craigmile *et al.* 2023). Furthermore, both Langevin approach and Bayesian methods demand substantial amounts of data for reliable estimation (Siegert, Friedrich & Peinke 1998; Rinn *et al.* 2016; Ryder *et al.* 2018). An alternative approach involves model-fitting techniques that maximize a likelihood function. This approach includes both the classical Euler inference scheme and a novel methodology pioneered by Aït-Sahalia (Aït-Sahalia 2002). It offers an attractive method that requires fewer data for reliable parameter estimation.

This paper presents a maximum likelihood estimation (MLE) approach for reconstructing the following one-dimensional Langevin model from time series data

$$dx = \mu(x;\theta)dt + \sigma(x;\theta)dW, \tag{1}$$

where $\mu(x;\theta)$ denotes the deterministic component of the system, referred to as the 'drift function' and $\sigma(x;\theta)$ represents the stochastic component, known as the 'diffusion function'. θ represents the parameter vector to be estimated via MLE and W refers to a Wiener process, under which the noise source dW, known as Brownian noise, is Gaussian and white (uncorrelated). The diffusion function $\sigma(x;\theta)$ weighs the impact of noise, reflecting the intensity of perturbations at state x. The noise in a diffusion model (1) is additive if

the diffusion function does not depend on the state x (i.e., it is constant in terms of state), otherwise, the noise is called multiplicative. The inference technique employed here is parametric meaning that a parametric form, with a single vector θ of parameters, for both the drift $\mu(x;\theta)$ and diffusion $\sigma(x;\theta)$ functions should be predefined and then the parameters are estimated using time series data through MLE.

In this study, we apply the classical inference of Langevin models using Euler methodology which we call 'Euler reconstruction'. This method requires data of high resolution which may be a significant challenge in fields such as ecology and climate science. To address this issue, we present an MLE scheme based on the groundbreaking work of Aït-Sahalia (Aït-Sahalia 2002) for univariate sparsely sampled data. The idea of Aït-Sahalia involves constructing an approximate conditional density, and therefore an approximate MLE or quasi MLE, of (1) using Hermite polynomials, so we call this procedure 'Hermite reconstruction'. An appealing feature of Hermite reconstruction is that it offers the highest accuracy among reconstruction algorithms while at the same time remaining computationally efficient (see Figure 1 in Aït-Sahalia's paper (Aït-Sahalia 2002) or the book by Jensen and Poulsen (Jensen & Poulsen 1999)). The superior accuracy of Hermite reconstruction is demonstrated in the case studies on simulated and real data presented in our tutorial (Examples 7-12).

To our knowledge, this paper is the first to provide an open-access MATLAB package for Hermite reconstruction and to demonstrate successful applications to ecosystem and climate data. One of our key techniques for addressing the underlying MLE problem is the use of a wide variety of spline models (De Boor & De Boor 1978) as representation of the unknown drift and diffusion functions. Splines offer two appealing features: ease of fitting and computational efficiency (for a detailed technical discussion of their superiority, see Appendix G). First, splines are flexible non-linear structures in terms of the state variable x making them valuable tools in situations where selecting an appropriate model is uncertain. Their flexibility stems from being constructed by smoothly joining polynomial pieces, enabling them to capture complex nonlinearities in the underlying data-generating process. Since the true form of these nonlinearities is unknown in practice conventional parametric models can only be appropriate when supported by strong

empirical evidence or theoretical justification (e.g., derived from first principles). Even when the true governing laws are known splines may still outperform them. For instance, in simulation case studies 7-11 of our tutorial spline models achieved lower objective values than the true parametric models under both Euler and Hermite reconstructions, indicating better fits. Second, splines are linear functions in terms of parameter vector θ. This fact significantly enhances the accuracy and speed of calculations. These dual properties—nonlinearity in the input and linearity in parameters—makes splines particularly well-suited for the MLE framework. These advantages are demonstrated across multiple examples in our tutorial, with technical details in Method's section. To distinguish this modeling technique from conventional 'parametric modeling' we refer to it as 'spline modeling'.

The remainder of the paper presents the steps of the analysis, demonstrates reconstruction of diffusion models for several simulated, ecological, and climate data and shows that the method succeeds even for rarified datasets. Supplementary materials include a mathematical appendix, and a tutorial to illustrating a broader range of the capabilities of the Euler and Hermite reconstructions using both parametric and spline models across different data types. These data types encompass typical time series data (i.e., single time series), replicate time series (multiple time series belonging to the same data-generating system), large datasets (where a well-mixed small fraction of data will be used instead of the entire dataset), datasets with missing values, or various combinations of these. In the reference (Arani *et al.* 2021), a glossary clarifies several technical mathematical terms used here.

Steps of the Method.

Step 1. Prepare the data: data standardization

In some real datasets, the scale (range) of the data can be very large. In such cases, data standardization, achieved by computing z-scores (subtracting the mean and dividing by the standard deviation), makes it easier to solve the MLE. This is because standardization helps to narrow down large search spaces, making them more manageable. Additionally, standardization brings the data to a common scale, centered at 0 with

small dispersion. This, in turn, makes it convenient to define a small region of parameter space for the MLE algorithm to search within especially for spline modeling (Step 4). For further discussion on data standardization, refer to section 8 of tutorial and Appendix G.

Step 2. Check the data requirements

There are three data requirements for a Langevin model which should be checked prior to performing the reconstruction (for a detailed discussion see section 6 of the tutorial). Firstly, data should be stationary, meaning that its statistical properties remain unchanged throughout the study period. If this assumption is violated, the data should be divided into smaller (possibly overlapping) periods where stationarity is assured. Reconstruction can then be carried out separately for each period, with the final system reconstruction obtained by interpolating the results. Secondly, data should be Markovian meaning that the future state of data, given the present state, should be independent of the entire past history of states. The smallest time scale at which Markovicity holds is called the 'Markov-Einstein' (ME) time scale. Reconstruction can, then, be performed on a rarified sample of data whose resolution matches the (ME) time scale (Friedrich et al. 2011) or on samples with lower resolutions. To estimate ME time scale, we fit an autoregressive (AR) model to the data and examine its order, say p. If the fitted AR model has order one ($p = 1$), this strongly suggests that the ME time scale equals the data's sampling interval, indicating that the dataset is Markovian. Conversely, if the AR model has an order greater than one ($p > 1$), the ME time scale is p times the data's sampling interval, meaning the dataset is not inherently Markovian. However, a rarified sample, taken every p^{th} data point, will exhibit Markovicity, and reconstruction should be performed on this rarified sample. Thirdly, it is essential to check the resolution of the rarified sample regarded now as our dataset to be analyzed. This is the subject of next step.

Step 3. Check the resolution of data: how high should the data resolution be?

How high should the data resolution be in order to be able to reconstruct the data-generating system? This is a question we should investigate prior to performing any reconstruction procedure. The answer depends

on the 'speed' or 'time scale' of the yet unknown system relative to sampling frequency of the data. To investigate the resolution of data the autocorrelation function of data should be examined and a quantity known as '*relaxation time*' τ_R should be estimated. As its name indicates, relaxation time is the time it takes for a process to get 'relaxed' or become 'statistically independent' of the starting state (Anteneodo & Queirós 2010; Honisch *et al.* 2012). We can roughly estimate relaxation time directly from data by fitting the exponential $\exp(-ct)$ to the initial lags of the data autocorrelation function, obtaining the estimates $\hat{c}$, and $\widehat{\tau_R} = 1/\hat{c}$ (Honisch *et al.* 2012) (refer to Appendix A for the details). Assuming Δ to be the data sampling interval we consider the following three cases.

***The first case:* Δ *being much smaller than* τ_R ($\Delta \ll \tau_R$)**

In this high-resolution regime we can safely apply simple reconstruction schemes like Euler scheme or Langevin approach (Rinn *et al.* 2016) (see Figure 1). Unfortunately, many real datasets are not sampled frequently enough to fall into this regime. Furthermore, some high-resolution data do not adhere to the Markov property, which is another data requirement (see Step 2). However, a rarified sample of such data may be Markovian at the expense of reduced resolution.

***The second case:* Δ *being approximately the same order of magnitude as* τ_R**

In theory, it may be possible to reconstruct the underlying system in this case using more sophisticated reconstruction algorithms (Anteneodo & Queirós 2010; Honisch *et al.* 2012). In practice, however, current reconstruction procedures typically perform reliably when the sampling interval does not exceed the relaxation time, i.e., $\Delta \leq \tau_R$. Consequently, in this work we consider $\Delta = \tau_R$ as the minimum resolution required for accurate data reconstruction. This resolution limit defines a critical resolution in practice (see Figure 1). In such cases (i.e., Δ not being small but still less than or equal to τ_R), a more accurate reconstruction procedure than the Euler scheme is often necessary. Here, Hermite reconstruction becomes essential (see Figure 1). Refer to Example 5, which showcases a dataset accurately reconstructed with high precision using Hermite reconstruction at a resolution matching the critical threshold τ_R.

The third case: Δ being much bigger than τ_R ($\Delta \gg \tau_R$)

In this case, consecutive measurements are almost independent. Therefore, the true dynamics is not reflected in such datasets, and reconstruction procedures are likely to fail in this 'independence limit' (Anteneodo & Queirós 2010) due to systematic errors termed 'finite time effects' in the literature (Honisch *et al.* 2012) (see Figure 1). Increasing the dataset size (i.e., the number of data points) does not resolve this issue—even a very large dataset remains ineffective.

Here, we provide a convention for categorizing data resolution into low- and high-resolution regimes when $\Delta \leq \tau_R$. Specifically, we classify a dataset as having high resolution if Δ falls in the interval $(0, 0.01\tau_R]$, and low-resolution if Δ falls in the interval $(0.01\tau_R,\ \tau_R]$. While the threshold τ_R has a theoretical foundation based on the autocorrelation structure of the data, the threshold $0.01\tau_R$ is suggested as a guideline. It is important to note that these resolution categories provide only approximate guidelines, as the relaxation time τ_R of the unknown data-generating system can only be estimated. Thus, this convention offers a general sense of the data resolution rather than a precise determination.

While Euler reconstruction is often suitable for high-resolution regime, Hermite reconstruction may be required for the low-resolution regime (see Figure 1). For real datasets extra caution is needed and in general we suggest Hermite reconstruction even when the resolution is high and use Euler reconstruction when the resolution is exceptionally high.

Figure 1. A schematic illustration of different regimes of resolution along with appropriate reconstruction procedures for each. High- and low-resolution data correspond to sampling intervals within the ranges $(0, 0.01\tau_R]$ and $(0.01\tau_R,\ \tau_R)$, respectively, where τ_R represents the relaxation time of the system which can be estimated from the

correlational information in the data. Euler reconstruction is suitable for high-resolution data, while Hermite reconstruction is necessary for low-resolution data. If the sampling interval exceeds τ_R, the data are considered too coarse and reconstruction may not be feasible.

Guidelines for implementing parametric and spline modeling

In parametric modeling, parametric forms for the drift and diffusion functions in the Langevin model (1) should be specified prior to embarking on MLE. For instance, in the Ornstein-Uhlenbeck model the parametric forms for the drift and diffusion functions are $\mu(x) = -\mu x$ and $\sigma(x) = \sigma$, respectively where $\theta = [\mu, \sigma]$ is the vector of parameters. Similarly, in the grazing model of May (May 1977) $\mu(x) = rx\left(1 - \frac{x}{K}\right) - \frac{\gamma x^2}{x^2+a^2}$, $\sigma(x) = \sigma$ where x represents the biomass of a plant population, $\theta = [r, K, \gamma, a, \sigma]$ is the vector of parameters in which, r is the growth rate, K is the carrying capacity, γ is the maximum grazing rate, a is the efficiency of the grazer, and σ is the intensity of environmental perturbations which is assumed to be constant (so, this is an additive model).

In spline modeling (De Boor & De Boor 1978), on the other hand, no specific model for drift and diffusion functions needs to be specified in the conventional sense. Instead, a rather sparse mesh across the data range, called 'knot sequence', is specified. Knots are the x-coordinates of points where the spline interpolation goes through and the values of the drift and diffusion spline functions at these knots serve as model parameters (see red stars in Figures 2-9). Simply put, splines are piecewise polynomials that are smoothly joined to construct a 'complex' functional form. Therefore, splines are 'flexible' structures which enable us to recover the unknown nonlinearities of drift function $\mu(x)$ and diffusion function $\sigma(x)$.

We commonly use quadratic or cubic splines, with cubic splines offering slightly better smoothing properties. However, Hermite reconstruction is significantly faster when using quadratic splines, especially for low-resolution or real-world datasets (see Appendix G for details. Also, see section 10 in the tutorial). In such cases, the reconstruction is performed using quadratic splines, and once complete, a cubic spline is

fitted to the result. Consequently, the final output provided by the package consists of cubic spline estimates for the drift and diffusion functions.

We select equidistant knots to minimize the sensitivity of the fitted spline to knot values, i.e., model parameters (De Boor & De Boor 1978) (details in Appendix G). Moreover, using a large number of knots is generally not advisable for several reasons. First, a large number of knots increases the complexity of the MLE problem, leading to numerous local maxima, and making the problem both challenging and time-consuming to solve. Second, in many practical scenarios datasets are small, and using a large number of knots can produce bumpy estimates for the drift and diffusion functions. Third, we often encounter unimodal or bimodal datasets, where the underlying system has either one equilibrium or three equilibria (two stable and one in the middle being unstable). In such cases, four knots are sufficient to estimate drift and diffusion functions qualitatively. For reasonably accurate quantitative results, eight knots are typically sufficient, as employed in many of our examples. However, in two cases (Example 5 and Example 8) with low-resolution data, we used seven knots to speed up parameters estimation in Hermite reconstruction.

After selecting a model (parametric or spline), a vector of lower bounds and a vector of upper bounds for the parameters should be specified for the optimization (MLE) to search within and find the optimal parameter values. All parameters associated with the diffusion function should be bounded in a way that ensures the diffusion function remains positive. For parametric models, the physics of the problem can provide insights to determine proper vectors of lower and upper bounds. For example, in the case of the May model, we know that all model parameters should be positive as they represent ecological quantities. For spline models selecting vectors of lower and upper bounds are convenient since we deal with stationary data. For instance, for the drift parameters, we can set all lower bounds to $-L$ and all upper bounds to L while for diffusion parameters we can set all lower bounds to 0 and all upper bounds to L where $L > 0$ should be big enough. In all the examples in this paper, we set $L = 10$ (although $L = 5$ was also sufficient). It is straightforward to verify whether the chosen L is sufficiently large: if any of the model parameters (knot values) approaches L closely, it suggests that L needs to be increased.

If a parametric model is preferred and it is uncertain to choose a proper model then it is advisable to select drift and diffusion models which contain constant, linear, quadratic, and higher order terms due to Taylor series expansion. An additive version of such a modeling is

$$dx = \{\alpha + Ax + Bx^2 + \ldots\}dt + \sigma dW\,, \tag{2}$$

The parameter A is particularly insightful as it is the sole determinant of stability of the deterministic part of (2). The model form in (2) is not directly suited for fitting to data. For convenience and ease of parameter estimation, data should be standardized first, and then the model (2) could be applied. Since, this model is linear in parameters, it is convenient to transform the estimated parameters back into their original scales by replacing the state variable x with its standardization $(x - m)/s$ and multiplying the right-hand side by s where m and s are the mean and standard deviation of the data, respectively.

Step 5. Euler reconstruction

If the data resolution falls within the high-resolution regime, the general Langevin model (1) can be approximated by a difference equation using the Euler-Maruyama discretization scheme (Gardiner 1985). This yields a closed-form approximation for the conditional distribution of model (1), which is typically unavailable in general and represents the primary challenge in the inference of Langevin models. This resulting closed form enables construction of an approximate likelihood function (quasi-MLE). From there, parameter estimation reduces to solving an optimization problem. For technical details, see Appendix D.

Step 6. Hermite reconstruction

If the data resolution falls within the low-resolution regime, Hermite reconstruction should be employed. Here, we briefly outline the approach; but for detailed mathematical explanations, refer to Appendices F, G, H, and I. A less technical discussion, along with numerous case studies, is provided in section 11 of the tutorial. Our MATLAB package implements Hermite reconstruction based on a refinement by (Bakshi & Ju 2005) of a methodology developed by (Aït-Sahalia 2002). The approach follows a two-phase algorithm.

In the first phase, Euler reconstruction is used to find an initial estimate $\hat{\theta}_{Euler}$ of parameter vector. In the second phase, $\hat{\theta}_{Euler}$ is improved using Hermite reconstruction.

Reconstructing low-resolution data is computationally demanding. The main challenge arises in the second phase, where the optimization problem involves a partially-defined objective function. As data resolution decreases, the algorithm should search within narrower regions in the parameter space. To overcome this, it first identifies a set of parameter vectors, we call 'legitimate points' (LP), at which the Hermite objective function has defined values. Subsequently, the algorithm utilizes these LPs and searches in the vicinity of $\hat{\theta}_{Euler}$ to find an improved vector of parameters $\hat{\theta}_{Hermite}$.

Our package supports a variety of spline types, including the commonly used cubic splines. The use of 'quadratic' splines can significantly enhance computational speed when data resolution is low. While both parametric and spline models can be used, spline modeling is generally preferable due to its superior accuracy and speed.

Examples with high-resolution data

Example 1 (Analyzing a dataset simulated from a linear model). Here, we reconstruct a high-resolution but rather small dataset with 20000 data points (Figure 2, left panel) generated from the Ornstein-Uhlenbeck model with drift function $\mu(x) = -\mu x$, diffusion function $\sigma(x) = \sigma$, parameter values $\mu = \sigma = 1$, and sampling interval $\Delta = 0.01$. Parameter estimation for this linear parametric model yields $\hat{\mu} = -1.0586$ and $\hat{\sigma} = 0.9953$ for this linear parametric model. We also apply spline reconstruction to the same dataset using eight equidistant knots (Figure 2, right panel).

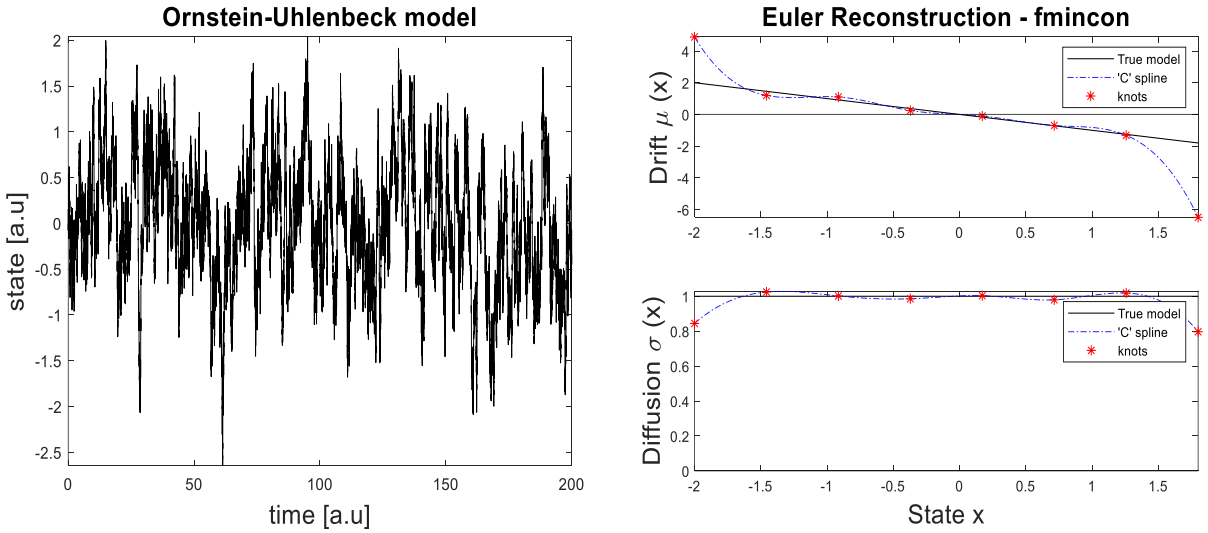

Figure 2. Illustration of spline reconstruction for a high-resolution dataset generated from a linear model. The left panel shows a dataset with 20000 data points simulated from the OU model with a sampling interval of $\Delta = 0.01$. The right panel illustrates the estimated cubic spline models (dot-dashed blue curves) for the drift and diffusion functions, reconstructed using 8 regularly spaced knots over the state space. The true drift and diffusion functions are shown in black for comparison. For simulated data, 'a.u' stands for arbitrary unit.

Example 2 (Analyzing a small fraction of a large dataset). In this example, we have a large high-resolution dataset with 10^6 data points, but aim to work with only a small fraction, just 1%, resulting in a small sample with 10^4 data points. As in Example1, the original dataset is generated from the OU model using the same parameters and sampling interval. In fact, the dataset in Example 1 corresponds to the first 20000 points of this larger dataset. Important to note is that both the original dataset and the smaller sample share the same resolution. Reconstructing a small fraction of a large dataset is necessary when reconstructing the original dataset is computationally expensive. A smaller but 'representative' sample can still provide accurate results. To this end, the sample should be a well-mixed random sample of 'data pairs', i.e., consecutive pairs of data points (see red and blue open circles in Figure 3, left panel). To achieve this we use stratified random sampling of data pairs, which provides better mixing than simple random sampling (Cochran 1977). Results may vary slightly depending on sample quality. For the sample illustrated in Figure

3 (left panel), parametric reconstruction yields $\hat{\mu} = -1.035$ and $\hat{\sigma} = 0.997$. Figure 3 (right panel) depicts

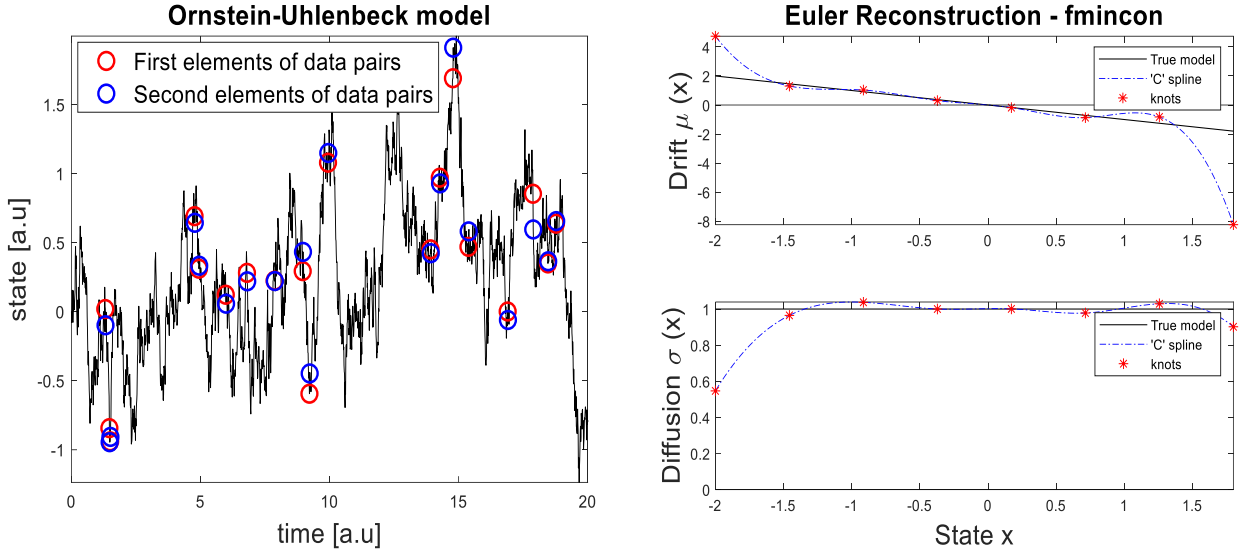

a spline reconstruction of the sample using 8 knots.

Figure 3. Illustration of spline reconstruction from a high-resolution random sample of a large dataset. For clarity, data are plotted only up to time $T = 20$, although the simulation extends to $T = 10^4$. The model parameters and sampling interval are identical to those used in Figure 1. In the left panel, the open red and blue circles represent 'data pairs' which are consecutive data points selected through stratified random sampling from the original dataset (depicted in black). These data pairs constitute a small but well-mixed fraction, comprising only 1% of the original dataset. The right panel displays a spline reconstruction of this sample using 8 equidistant knots.

Example 3 (Analyzing a dataset simulated from a nonlinear model). In this example, a dataset simulated from the overgrazed model of May (Figure 4, left panel), with drift function $\mu(x) = rx\left(1 - \frac{x}{K}\right) - \frac{\gamma x^2}{x^2+a^2}$ and diffusion function $\sigma(x) = \sigma$, is reconstructed. This dataset consists of 10^5 data points with sampling interval of $\Delta = 0.01$. The parameter values are $r = 1.01, K = 10, \gamma = 2.75, a = 1.6, \sigma = 0.4$. Under these parameters, the deterministic model of May (i.e., without noise) exhibits over-grazed and under-grazed alternative vegetation states (Figure 4, top right panel). Unlike the dataset in Example1, the May model is nonlinear with respect to both the parameters K and a as well as the state variable x.

Therefore, a longer dataset is needed to effectively capture transitions and timescales of state shifts between alternative basins of attractions. Nonetheless, we were able to estimate the model parameters with reasonable accuracy as $\hat{r} = 1.1805, \hat{K} = 9.8416, \hat{\gamma} = 3.1242, \hat{a} = 1.5279, \hat{\sigma} = 0.3997$. Figure 4, right panel, on the other hand, illustrates a cubic spline reconstruction of the dataset.

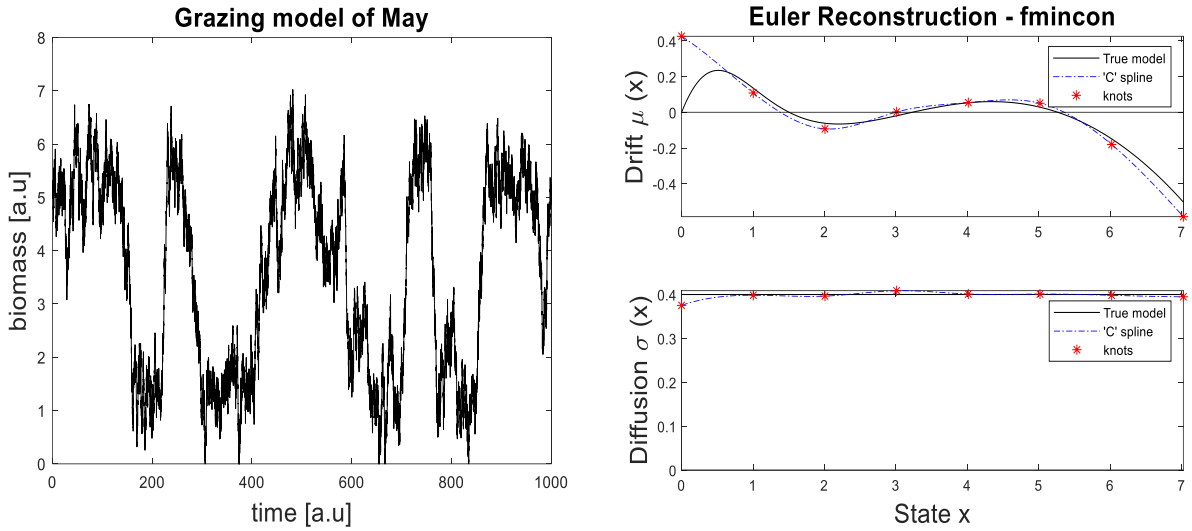

Figure 4. Illustration of spline modeling for a high-resolution dataset generated from a nonlinear model. The left panel depicts 10^5 data points simulated from the overgrazed model of May with sampling interval $\Delta = 0.01$. The right panel illustrates the estimated cubic spline models (dot-dashed blue curves) for both the drift and diffusion functions, using eight regularly spaced knots across the state space. For comparison, the true drift and diffusion functions are displayed as solid black curves.

Example 4 (Analyzing an ecological dataset). In this example, we reconstruct a high-resolution ecological dataset. The data represent an index of Cyanobacteria biomass, measured as phycocyanin concentrations in the Lake Mendota (Carpenter *et al.* 2020). Measurements were collected at one-minute intervals during the summer thermal stratification of 2011, a period known for common Cyanobacterial blooms (Figure 5, left panel). For further details, refer to (Arani *et al.* 2021; Magnuson, Carpenter & Stanley 2023).

This dataset does not meet a key data requirement, as it lacks Markov property, indicating strong correlations at the recorded time scale. However, a rarified sample of the dataset, constructed by selecting every fourth data point (still preserving high resolution), does exhibit Markovian behavior. Therefore, we applied Euler reconstruction using an additive spline model to this rarified sample (Figure 5, right panel, blue curve). However, since this is a real dataset, we also performed Hermite reconstruction (Figure 5, right panel, black curve). While both results are similar, the Hermite reconstruction provides a better fit, particularly in accurately locating the repellor, which is crucial for assessing the ecological resilience.

This example highlights the practical value of spline reconstruction for real-world data, where selecting an appropriate parametric model is difficult. In such cases, spline modeling provides a flexible and effective alternative.

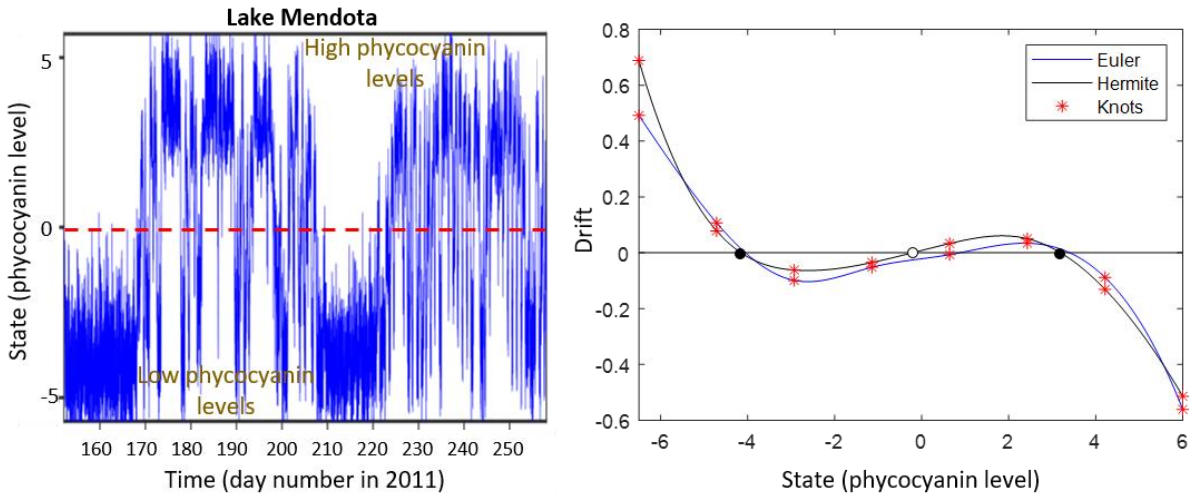

Figure 5. Illustration of spline modeling for a high-resolution ecological dataset. The left panel illustrates high-resolution cyanobacterial biomass measurements, taken at one-minute intervals, from lake Mendota. While the dataset does not satisfy the Markov property, a rarified sample constructed by selecting every fourth data point satisfies this data requirement. In the right panel, cubic spline modeling is applied to the rarified sample to estimate the drift functions with respect to Euler and Hermite reconstruction with the later giving a better fit especially in locating the repellor position. The estimated noise levels are 0.4396 (Euler) and 0.4567 (Hermite), respectively. The dataset is publicly available online (Magnuson, Carpenter & Stanley 2023) at the URL https://doi.org/10.6073/pasta/fc8bd96677405945024ad708003be1fc

Examples with low-resolution data

Example 5 (Analyzing a minimally resolved low-resolution dataset). Here, we reconstruct a dataset generated from the OU model using the same model parameters as in Example 1, i.e., $\mu = \sigma = 1$. This dataset is identical to the one in Example 1, but in that case, we only used the first 20000 data points. Although the original dataset contains 10^6 data points, we select every 100^{th} data points, resulting in a dataset with 10^4 data points. The resulting rarified dataset has the lowest allowable resolution as its sampling interval ($\Delta = 1$) equals its relaxation time (see red dashed arrow in Figure 1). In practice it might still be possible to exceed this threshold a bit. Nonetheless, as a proof of concept, we show that it is possible to estimate the model parameters with high accuracy for this poor dataset by using Hermite reconstruction which is more accurate.

First, we applied a parametric Hermite reconstruction and estimated the model parameters with remarkable accuracy: $\hat{\mu} = -0.99683$ and $\hat{\sigma} = 0.99489$. Next, to implement the spline reconstruction, we used 'quadratic' splines (rather than the more common cubic splines) for the Hermite reconstruction, significantly reducing computational time and enhancing the likelihood of successful parameter estimation. This choice is rooted in the nature of Hermite reconstruction algorithm (as detailed in Appendices F, G, and particularly H). Once again, we could recover the true drift and diffusion functions with great accuracy. The Hermite reconstruction improved upon the outcomes of Euler reconstruction (Figure 6). For this extremely low-resolution dataset, we used 7 equidistant knots for both the drift and diffusion functions, compared to 8 knots used in other examples, to speed up the calculations. For Hermite reconstruction of very low-resolution data we need to be economical with respect to the number of knots as more knots means more model parameters. The major challenge for such 'highly damaged' datasets is to identify few candidate 'legitimate solutions' within the parameter space (see Step 6 in Methods section), to initiate optimization. Alternatively, one could consider using simpler additive models (see Example 7 or Example 9 in the tutorial).

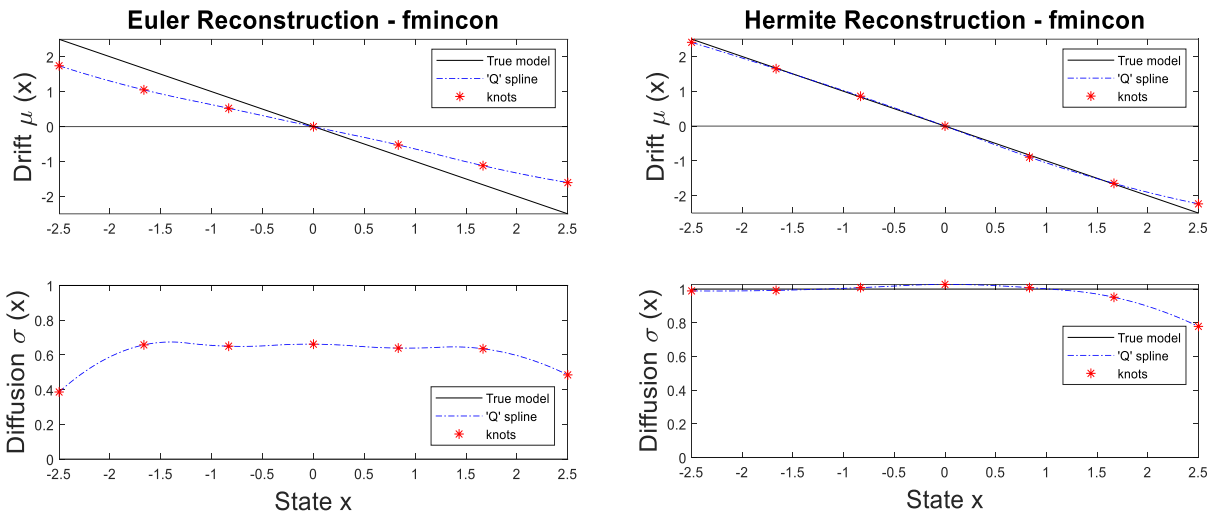

Figure 6. Illustration of spline reconstruction applied to an extremely low-resolution dataset generated from a linear model using Euler and Hermite reconstructions. The left panel illustrates Euler estimated quadratic spline models (dot-dashed blue curves) for both the drift and diffusion functions, using 7 regularly spaced knots across the state space, alongside the true drift and diffusion functions (black curves). Similarly, the right panel illustrates Hermite estimated quadratic spline models (dot-dashed blue curves) alongside the true model (black curves).

Example 6 (Analyzing a dataset simulated from a nonlinear model). In this example, we reconstruct the same dataset as in Example 3, but with a resolution that is 300 times lower, resulting in a low-resolution

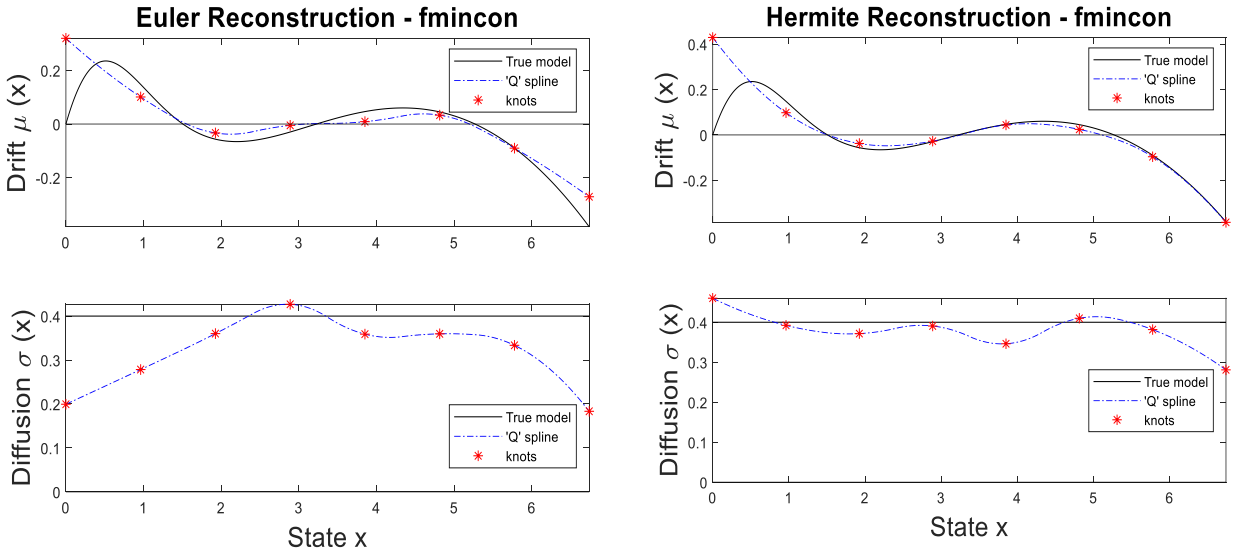

Figure 7. Illustration of Hermite and Euler reconstructions applied to a low-resolution dataset generated from a nonlinear model. The left panel illustrates Euler estimated quadratic spline models (dot-dashed blue curves) for both the drift and diffusion functions, using 8 regularly spaced knots across the state space, alongside the true drift and diffusion functions (black curves). The right panel illustrates Hermite estimated quadratic spline models (dot-dashed blue curves) for both the drift and diffusion functions, also using 8 regularly spaced knots over the state space, alongside the true drift and diffusion functions (black curves).

dataset. To reconstruct it, we apply Hermite reconstruction using quadratic splines. Despite the dataset's low-resolution, Hermite reconstruction yields accurate results in capturing the nonlinearities of the drift and diffusion functions (Figure 7, right panel), outperforming Euler reconstruction (Figure 7, left panel).

Example 7 (Analyzing a replicate dataset). In this example, we reconstruct a low-resolution dataset that differs from datasets analyzed so far. Instead of a single uninterrupted time series, the dataset consists of three separate fragments (highlighted in black, blue, and orange in Figure 8, top panel). Such data are common in many practical applications, making it important to develop methods for their reconstruction as well. The fragments are simulated from the grazing model of May. Each replicate is initialized at $x_0 = 8$ biomass and continues until perturbations drive it toward 0 biomass. In order to remove the impact of transient effects, the initial 5% of each replicate is discarded, and to generate a low-resolution dataset, every 30^{th} data point is selected.

The resulting dataset not only has low resolution but also a short total length of just 471 data points (see solid dots in Figure 8, top panel). Reconstructing such data accurately is a significant challenge, and in such cases we aim to understand the qualitative, rather than quantitative, characteristics of the data-generating system. To address this, we fitted an additive quadratic spline model to this poor-quality dataset. While Euler reconstruction produced inaccurate results (Figure 8, bottom left panel), Hermite reconstruction is somewhat better (Figure 8, bottom right panel). Notably, Euler reconstruction failed to detect the presence of under-grazed states in the entire dataset, due to its low data density. In contrast, Hermite reconstruction was able to identify these states, at least qualitatively.

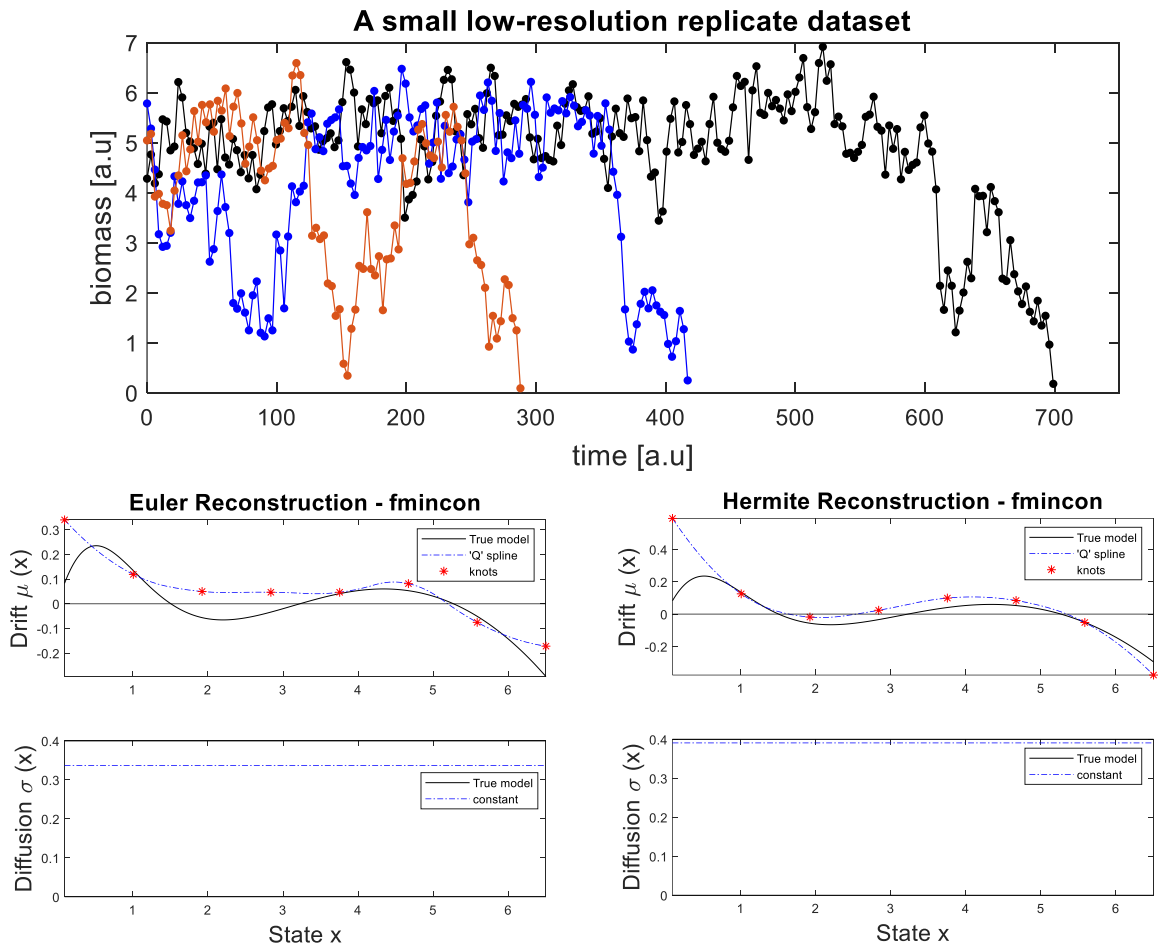

Figure 8. Illustration of Hermite and Euler reconstructions applied to a low-resolution and fragmented dataset. The top panel illustrates three low-resolution separate segments. These segments are generated using May model, where all segments initialize at $x_0 = 8$ biomass and continue until perturbations drive them toward 0 biomass. To remove transient effects, the first 5% of each segment is discarded. Datasets is then rarified by selecting every 30th data point in each segment. The bottom left and bottom right panels are produced similarly to those in Figure 7.

Example 8 (Analyzing a small climate dataset). In this example, a low-resolution climate dataset is reconstructed. The dataset, a δ^{18}O record from the North Greenland Ice Core Project (NGRIP) (2004), serves as a proxy for the temperature of the northern hemisphere (Kwasniok & Lohmann 2009), spanning the last 120 thousand years with a resolution of 20 years (Andersen *et al.* 2007). However, this dataset fails to meet two key data requirements outlined in Step2. Initially, the dataset exhibits non-stationarity, although

it stabilizes within the period from 70 to 20 thousand years before the present (see Figure 9, top panel). During this epoch, the northern hemisphere climate witnessed alternating colder (stadial) and warmer (interstadial) states, attributed to Dansgaard–Oeschger (DO) events (Dansgaard *et al.* 1993). Within the specified time frame, the majority of DO events, from DO2 to DO18 out of a total of 25 DO events, occurred (2004). Secondly, the dataset lacks the Markov property, yet a rarified sample, with every other point demonstrates Markovian behavior approximately (refer to section 6.3 of the tutorial for further details).

Since this dataset has a low resolution, Hermite reconstruction is deemed suitable. Here, we employ quadratic spline modeling. Figure 9 (bottom panels) illustrates the outcomes of Euler and Hermite reconstructions. Additionally, we introduce a n important quantity known as '*effective potential*' (For

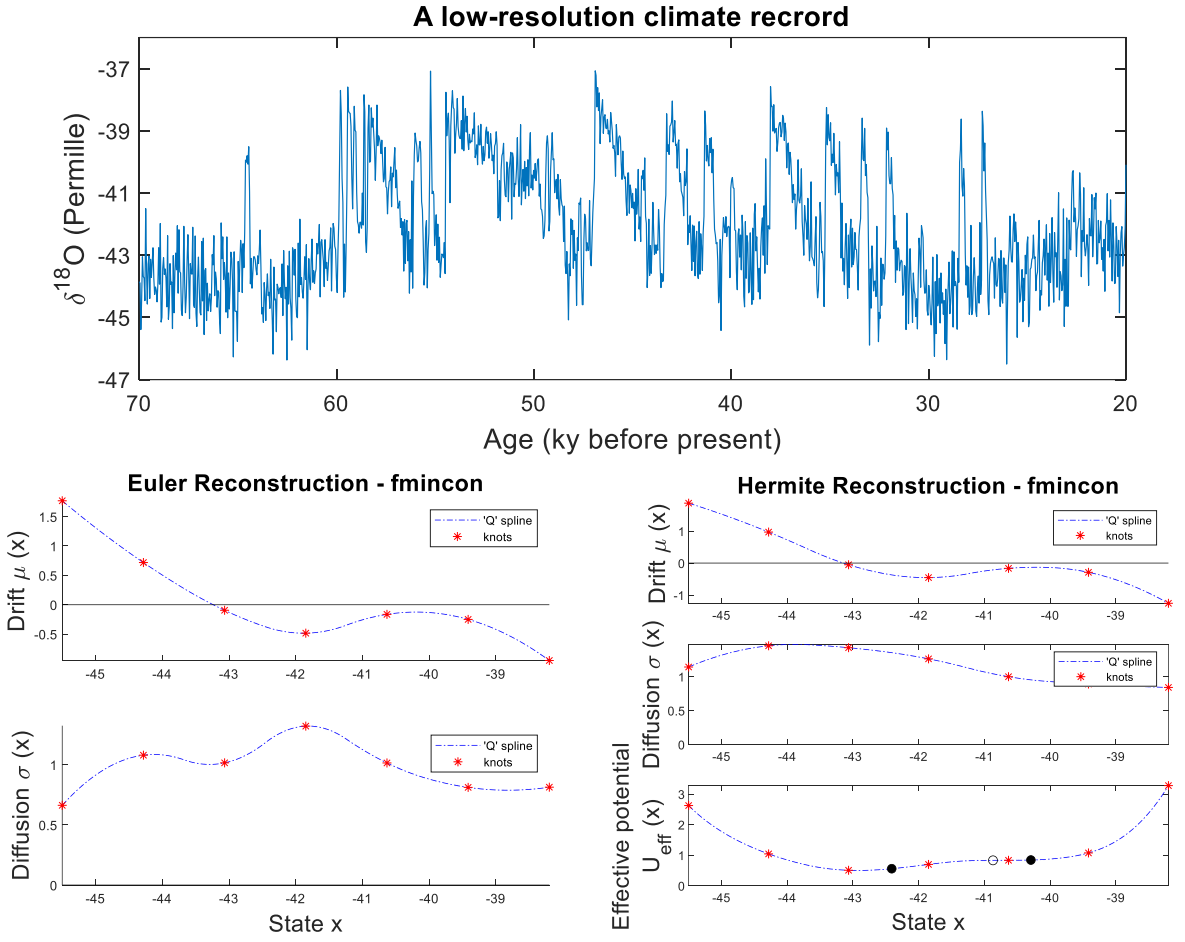

Figure 9. Illustration of Hermite and Euler reconstructions applied to a low-resolution climate dataset. The top panel illustrates a δ^{18}O climate record extending from 70 to 20 thousand years before the present from NGRIP. This dataset is used as a proxy for the temperature of the northern hemisphere which shows that the northern hemisohere climate alternated between cold stadial and warmer interstadial alternative climate states. In this time period the majority of Dansgaard-Oescher events occurred (see the labels 2 to 18). The description for bottom left and right panels are similar to that in Figure 6 or Figure 7. However, in the bottom right panel the effective potential is also depicted. Effective potential is useful to see whether there are alternative stable states in the dataset which is the case in this dataset (the solid dots represent alternative climate states of stadial and interstadial states separated by the open circle in between).

technical details refer to section 10.5 in the tutorial). Unlike deterministic systems or stochastic but additive systems (see Example 4), where equilibria can be identified solely by the drift function, this is not the case for stochastic multiplicative model. For such systems effective potential should be used which is a quantity that incorporates information from both drift and diffusion functions. The minima of effective potential indicate the location of alternative stable states of stadial and interstadial states (solid dots in Figure 9, bottom right panel) which are separated by a repellor (i.e., the maximum of the effective potential) in between (open circle in Figure 9, bottom right panel).

Discussion

System reconstruction is essential for ecosystem analysis, prediction and, management. In particular, reconstruction largely involves modeling real-world phenomena which are subject to environmental perturbations through stochastic dynamical systems, such as Langevin systems. An important application of such stochastic systems is that they are essential to quantify ecosystem resilience. Unlike stability, resilience requires the estimation of not only the internal dynamical forces (i.e., drift function) but also external environmental perturbations (i.e., diffusion function). By estimating both the drift and diffusion elements within the Langevin framework one can quantify ecological resilience using indicators such as exit or survival times. Another example that highlights the importance of system reconstruction is the

458 accurate estimation of critical transitions. Early warning signals (EWS) (Scheffer 2009; Scheffer *et al.* 2009)
459 are often used to assess whether a system is approaching a tipping point. However, EWS typically provide
460 'relative' information about proximity to a critical transition. In contrast, system reconstruction can
461 systematically recover the underlying bifurcation structure (e.g., hysteresis curve) of the system.

462 By delineating a systematic approach encompassing data preparation, model selection, and reconstruction
463 techniques, we furnish researchers with a practical guide and MATLAB package for analyzing diverse
464 univariate datasets. The methods and examples presented in this paper furnish valuable insights into the
465 reconstruction of Langevin systems from datasets of varying resolutions. Our discussion of data
466 requirements is fundamental for reconstructing real datasets. We acknowledge the challenges posed by real
467 datasets that do not meet these requirements and propose strategies such as data division (Example 9) or
468 rarified sampling (Example 4 and Example 9) to address these limitations. We introduced two different
469 modeling strategies: parametric versus spline modeling. The choice between parametric and spline modeling
470 depends on the nature of the dataset and the researcher's familiarity with the underlying dynamics, including
471 prior empirical knowledge. While parametric models offer interpretability with respect to model form,
472 spline models provide flexibility in capturing unknown model nonlinearities, rendering them particularly
473 suitable when the true model is uncertain. In general, we recommend to use spline modeling. Furthermore,
474 without incorporation of splines, addressing Hermite reconstruction for low-resolution data pose
475 considerable challenges.

476 The examples presented illustrate the application of our methodology to diverse datasets (e.g., high-
477 resolution versus low-resolution data, Markov versus non-Markov data, typical versus replicate data, big
478 data, etc.), spanning from simulated data to ecological data and climate records. These examples underscore
479 the efficacy of both Euler and Hermite reconstruction techniques, demonstrating their utility across different
480 resolutions and system complexities. Hermite reconstruction proves to be particularly valuable for low-
481 resolution datasets, offering higher accuracy compared to Euler reconstruction. This is particularly

important in the fields of ecology and climate sciences, as many ecological and climate datasets have lowresolution.

Overall, our approach furnishes a systematic framework for reconstructing complex systems from observational data. While the examples provided demonstrate the efficacy of our methodology, further research is warranted to explore its applicability to other domains and datasets, especially those generated by more complex processes than Langevin models, such as diffusion-jump models (Gardiner 1985; Bandi & Nguyen 2003; Bandi & Phillips 2003) or models driven by Lévy noise (Siegert & Friedrich 2001; Li *et al.* 2022). Additionally, ongoing efforts to enhance computational efficiency and address computational challenges associated with multivariate Hermite reconstruction (Aït-Sahalia 2002) promise to advance the field further.

References

(2004) High-resolution record of Northern Hemisphere climate extending into the last interglacial period. *Nature,* **431,** 147-151.

Aït-Sahalia, Y. (2002) Closed-form likelihood expansions for multivariate diffusions. National Bureau of Economic Research Cambridge, Mass., USA.

Aït-Sahalia, Y.J.E. (2002) Maximum likelihood estimation of discretely sampled diffusions: a closed-form approximation approach. **70,** 223-262.

Andersen, K.K., Bigler, M., Buchardt, S.L., Clausen, H.B., Dahl-Jensen, D., Davies, S.M., Fischer, H., Goto-Azuma, K., Hansson, M.E. & Heinemeier, J. (2007) Greenland Ice Core Chronology 2005 (GICC05) and 20 year means of oxygen isotope data from ice core GRIP. *(No Title)*.

Anteneodo, C. & Queirós, S.D. (2010) Low-sampling-rate Kramers-Moyal coefficients. *Physical Review E—Statistical, Nonlinear, and Soft Matter Physics,* **82,** 041122.

Arani, B.M., Carpenter, S.R., Lahti, L., Van Nes, E.H. & Scheffer, M. (2021) Exit time as a measure of ecological resilience. *Science,* **372,** eaay4895.

Bakshi, G. & Ju, N.J.T.J.o.B. (2005) A Refinement to Aït-Sahalia's (2002)"Maximum Likelihood Estimation of Discretely Sampled Diffusions: A Closed-Form Approximation Approach". **78,** 2037-2052.

Bandi, F.M. & Nguyen, T.H. (2003) On the functional estimation of jump–diffusion models. *Journal of Econometrics,* **116,** 293-328.

Bandi, F.M. & Phillips, P.C. (2003) Fully nonparametric estimation of scalar diffusion models. *Econometrica,* **71,** 241-283.

Bjørnstad, O.N. & Grenfell, B.T. (2001) Noisy clockwork: time series analysis of population fluctuations in animals. *Science,* **293,** 638-643.

Bolker, B.M., Gardner, B., Maunder, M., Berg, C.W., Brooks, M., Comita, L., Crone, E., Cubaynes, S., Davies, T. & de Valpine, P. (2013) Strategies for fitting nonlinear ecological models in R, AD M odel B uilder, and BUGS. *Methods in Ecology and Evolution,* **4,** 501-512.

Carpenter, S.R., Arani, B.M., Hanson, P.C., Scheffer, M., Stanley, E.H. & Van Nes, E. (2020) Stochastic dynamics of Cyanobacteria in long-term high-frequency observations of a eutrophic lake. *Limnology and Oceanography Letters,* **5,** 331-336.

Chen, Y., Angulo, M.T. & Liu, Y.Y. (2019) Revealing complex ecological dynamics via symbolic regression. *BioEssays,* **41,** 1900069.

Cochran, W.G. (1977) Sampling techniques. *Johan Wiley & Sons Inc*.

Connell, J.H. & Sousa, W.P. (1983) On the evidence needed to judge ecological stability or persistence. *The American Naturalist,* **121,** 789-824.

Craigmile, P., Herbei, R., Liu, G. & Schneider, G. (2023) Statistical inference for stochastic differential equations. *Wiley Interdisciplinary Reviews: Computational Statistics,* **15,** e1585.

Dansgaard, W., Johnsen, S.J., Clausen, H.B., Dahl-Jensen, D., Gundestrup, N.S., Hammer, C.U., Hvidberg, C.S., Steffensen, J.P., Sveinbjörnsdottir, A. & Jouzel, J. (1993) Evidence for general instability of past climate from a 250-kyr ice-core record. *Nature,* **364,** 218-220.

De Boor, C. & De Boor, C. (1978) *A practical guide to splines*. springer-verlag New York.

Freedman, D.A. (1963) On the asymptotic behavior of Bayes' estimates in the discrete case. *The Annals of Mathematical Statistics,* **34,** 1386-1403.

Freedman, D.A. (1965) On the asymptotic behavior of Bayes estimates in the discrete case II. *The Annals of Mathematical Statistics,* **36,** 454-456.

Friedrich, R., Peinke, J., Sahimi, M. & Tabar, M.R.R.J.P.R. (2011) Approaching complexity by stochastic methods: From biological systems to turbulence. **506,** 87-162.

Gardiner, C.W. (1985) *Handbook of stochastic methods*. springer Berlin.

Golightly, A. & Wilkinson, D.J. (2011) Bayesian parameter inference for stochastic biochemical network models using particle Markov chain Monte Carlo. *Interface focus,* **1,** 807-820.

Guarini, J.-M. & Coston-Guarini, J. (2024) Alternate Stable States Theory: Critical Evaluation and Relevance to Marine Conservation. *Journal of Marine Science and Engineering,* **12,** 261.

Hilborn, R. & Mangel, M. (2013) *The ecological detective: confronting models with data (MPB-28)*. Princeton University Press.

Honisch, C., Friedrich, R., Hörner, F. & Denz, C. (2012) Extended Kramers-Moyal analysis applied to optical trapping. *Physical Review E—Statistical, Nonlinear, and Soft Matter Physics,* **86,** 026702.

Janse, J., Scheffer, M., Lijklema, L., Van Liere, L., Sloot, J. & Mooij, W. (2010) Estimating the critical phosphorus loading of shallow lakes with the ecosystem model PCLake: sensitivity, calibration and uncertainty. *Ecological Modelling,* **221,** 654-665.

Jensen, B. & Poulsen, R. (1999) *A comparison of approximation techniques for transition densities of diffusion processes*. Citeseer.

Kwasniok, F. & Lohmann, G. (2009) Deriving dynamical models from paleoclimatic records: Application to glacial millennial-scale climate variability. *Physical Review E—Statistical, Nonlinear, and Soft Matter Physics,* **80,** 066104.

Li, Y., Lu, Y., Xu, S. & Duan, J. (2022) Extracting stochastic dynamical systems with α-stable Lévy noise from data. *Journal of Statistical Mechanics: Theory and Experiment,* **2022,** 023405.

Magnuson, J.J., Carpenter, S.R. & Stanley, E.H. (2023) North Temperate Lakes LTER: High Frequency Data: Meteorological, Dissolved Oxygen, Chlorophyll, Phycocyanin-Lake Mendota Buoy 2006-current.

May, R.M. (1977) Thresholds and breakpoints in ecosystems with a multiplicity of stable states. *Nature,* **269,** 471-477.

Rinn, P., Lind, P.G., Wächter, M. & Peinke, J.J.a.p.a. (2016) The Langevin Approach: An R Package for Modeling Markov Processes.

Ryder, T., Golightly, A., McGough, A.S. & Prangle, D. (2018) Black-box variational inference for stochastic differential equations. *International Conference on Machine Learning*, pp. 4423-4432. PMLR.

Scheffer, M. (2009) *Critical transitions in nature and society*. Princeton University Press.

565 Scheffer, M., Bascompte, J., Brock, W.A., Brovkin, V., Carpenter, S.R., Dakos, V., Held, H., Van Nes, E.H.,
566 Rietkerk, M. & Sugihara, G.J.N. (2009) Early-warning signals for critical transitions. **461,** 53.
567 Scheffer, M., Carpenter, S., Foley, J.A., Folke, C. & Walker, B.J.N. (2001) Catastrophic shifts in ecosystems.
568 **413,** 591.
569 Scheffer, M. & Carpenter, S.R. (2003) Catastrophic regime shifts in ecosystems: linking theory to
570 observation. *Trends in ecology & evolution,* **18,** 648-656.
571 Siegert, S., Friedrich, R. & Peinke, J.J.a.p.c.-m. (1998) Analysis of data sets of stochastic systems.
572 Siegert, S. & Friedrich, R.J.P.R.E. (2001) Modeling of nonlinear Lévy processes by data analysis. **64,** 041107.

573

574

575